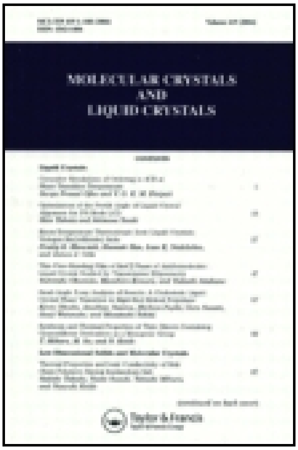

Molecular Crystals and Liquid Crystals
Publication details, including instructions for authors and subscription information:
http://www.tandfonline.com/loi/gmcl16

Characterization of the Phases in Centrifuged Mesophase Pitches

L. S. Singer [a] , I. C. Lewis [a] & R. A. Greinke [a]
[a] Union Carbide Corporation, Carbon Products Division, Parma Technical Center, P. O. Box 6116, Cleveland, Ohio, 44101

Version of record first published: 20 Apr 2011.

To cite this article: L. S. Singer , I. C. Lewis & R. A. Greinke (1986): Characterization of the Phases in Centrifuged Mesophase Pitches, Molecular Crystals and Liquid Crystals, 132:1-2, 65-79

To link to this article: http://dx.doi.org/10.1080/00268948608079529

Mol. Cryst. Liq. Cryst., 1986, Vol. 132, pp. 65–79
0026-8941/86/1322-0065/$20.00/0

Printed in the United States of America

Characterization of the Phases in Centrifuged Mesophase Pitches

L. S. SINGER, I. C. LEWIS, and R. A. GREINKE

Union Carbide Corporation, Carbon Products Division, Parma Technical Center, P. O. Box 6116, Cleveland, Ohio 44101

(*Received June 21, 1985*)

Mesophase pitches derived from petroleum, coal tar, and naphthalene have been separated into their isotropic and anisotropic phases by high-temperature centrifugation. The separated phases have been characterized by determining their elemental constitutions, densities, solubilities, glass transition temperatures, molecular weight distributions, and X-ray and EPR spectra. The data demonstrate the sensitivity of mesophase formation in carbonaceous pitches to molecular structure and distribution.

Keywords: centrifugation, discotic liquid crystals, mesophase pitch, molecular weight distribution, phase separation

INTRODUCTION

The occurrence of a mesophase state during the thermal transformation of carbonaceous materials to carbon is now widely recognized.[1] This mesophase is observed to form when complex aromatic mixtures (pitch) or individual reactive aromatic compounds are heat-treated within the temperature range 350°–500°C.[1] The carbonaceous mesophase generally develops initially as anisotropic spherules which precipitate from the original isotropic pitch phase. These spherules are composed of aromatic molecules which are stacked in parallel layers but with surface orientations which can vary depending on the nature of the material.[2] As the heat-treatment progresses, the spherules coalesce to form large bulk anisotropic regions which separate from the lower density isotropic pitch phase and slowly settle. The carbonaceous mesophase is known to have the characteristics of a discotic nematic liquid crystal.[3] The nematic liquid crystalline phase in pitch has also been shown by magnetic orientation and related experiments to exhibit uniaxial-negative optical behavior.[4-5]

From a number of general discussions of mesophase pitch,[1,3,6-9] it is clear that the development of mesophase in pitch requires polymerization of the aromatic components to a sufficient molecular size. Physical factors, including concentration and mutual solubilities, are also known to be important in controlling mesophase development in pitch.[10] However, the detailed chemical nature of the carbonaceous mesophase and its phase relationships with the isotropic pitch are still poorly understood.

The objective of this study was to clarify the physical properties and chemical composition of the co-existing anisotropic and isotropic phases in mesophase pitch. In order to achieve this objective, the two phases of several different mesophase pitches were separated by the use of high-temperature centrifugation. The apparatus and general procedures employed are described in a separate publication.[11] The mesophase pitches studied were prepared from conventional petroleum and coal tar pitches and from the aromatic hydrocarbon naphthalene. The separate phases of each material were characterized by a number of physical and chemical techniques. The results clarify considerably both the chemical and physical nature of the carbonaceous mesophase and the coexistent isotropic phase.

EXPERIMENTAL PROCEDURES

A. Preparation of mesophase pitches

Mesophase pitches were prepared by heat-treating solid-free commercial petroleum and coal tar pitches at 350°–400°C in an inert atmosphere. The naphthalene-derived mesophase pitch was prepared by heat-treating a pitch obtained by pyrolysis of naphthalene under pressure[12] at 420°C for five hours under nitrogen.

B. Centrifuging procedures

The centrifuge apparatus, which is a modification of that reported by Friedman,[13] is described in detail in a separate publication.[11] The three mesophase pitch materials described in this paper were centrifuged at temperatures between 300°C and 400°C employing a special sequence of heating and cooling.[11] Such a procedure was necessary to prevent disruption of the isotropic-anisotropic phase interface due to rapid evolution of dissolved volatiles during cooling. An example of the isotropic-anisotropic phase interface in a properly centrifuged petroleum mesophase pitch is shown in Figure 1, which will be discussed in Section C.

The samples for phase separation and analysis were contained in evacuated and nitrogen-filled (approximately 0.9 atm. N_2) sealed Pyrex sample tubes of 15 mm O.D. The centrifuging procedure for the petroleum and coal tar pitches was as follows:

1. Samples spun at 2600 rpm (500–700 g's) throughout the run.
2. Spinning samples heated to 400°C over a 20-minute period, followed by a one-hour hold at 400°C.
3. Spinning samples cooled to 300°C over a ten-minute period and held at 300°C for 20 minutes.
4. Spinning samples reheated to 400°C and held for one-half hour.
5. Samples cooled to room temperature while spinning.

The procedure for the naphthalene mesophase pitch was similar except that the highest centrifuging temperature was 390°C rather than 400°C.

After centrifuging and cooldown, the tubes were carefully broken and the solid sample billets removed essentially intact. The phases,

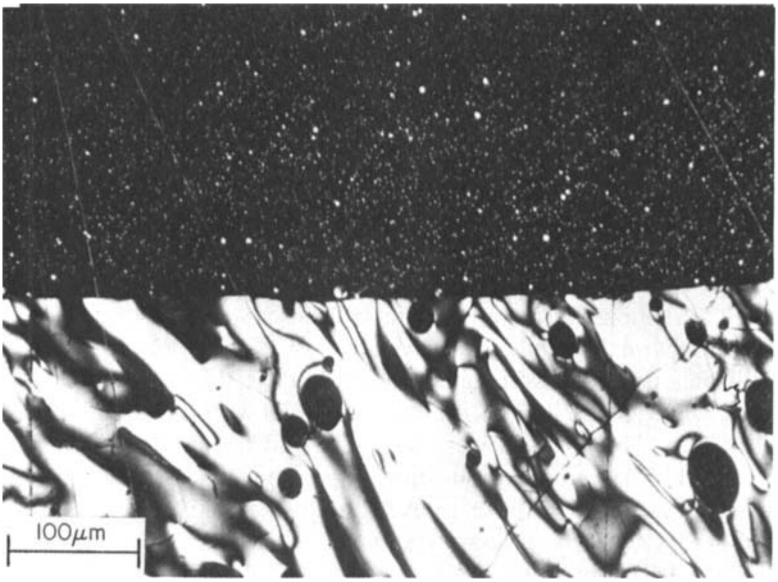

FIGURE 1 Anisotropic-isotropic phase interface in the centrifuged petroleum mesophase pitch in Table I.

which were easily apparent visually, fractured quite cleanly at the interfaces and were thus straight-forward to separate. Any questionable pieces near the interface region were discarded.

C. Characterization techniques

1. *Density Measurements*—Helium densities were determined on all of the samples utilizing a Beckman helium pycnometer apparatus.

2. *Elemental Analysis*—The C, H and N measurements were obtained on a Perkin-Elmer 240-C CHNO Elemental Analyzer. The S determinations were made by X-ray using a General Electric Model XRD-55 fluorescence spectrograph.

3. *Solubility*—The solubility of the pitches and separated phases were obtained by Soxhlet extraction using pyridine and toluene as solvents.

4. *Differential Scanning Calorimetry* (*DSC*)—The DSC measurements were made using a DuPont Model 990 Thermal Analyzer with a DSC attachment. The sample size was about 30 mg and the heating rate was programmed at 20°C/minute using an inert argon atmosphere. Glass transitions were very well defined for the separated isotropic phases and less well-defined for the anisotropic phases. The softening behavior was, therefore, also examined using thermomechanical analysis (TMA) to confirm the DSC results.

5. *Thermomechanical Analysis* (*TMA*)—Thermomechanical analysis measurements were made on all samples using the penetration mode of a Perkin Elmer Model TMS-1 Thermomechanical Analyzer, a slow flow of helium, and a heating rate of 10°C/minute.

6. *Thermogravimetric Analysis* (*TGA*)—The weight losses to 1000°C were determined with a DuPont 951 Thermal Analyzer using a sample size of 30 mg, an argon atmosphere at a flow rate of 100 ml/min and a heating rate of 10°C/minute.

7. *X-ray Diffraction*—The X-ray diffraction spectra were recorded using a Siemens X-ray Spectrometer at a scan rate of 1°/minute.

8. *Electron Paramagnetic Resonance* (*EPR*)—Room temperature EPR measurements were made employing the IBM Instruments Model ER/200D-SRC EPR Spectrometer equipped with the ASPECT 2000 computer. The samples were all evacuated to eliminate O_2-broadening and relaxation complications. Spin concentrations were determined by digital double integration utilizing single crystals of $CuSO_4{\cdot}5H_2O$ as the primary standard.

Since EPR spin-lattice relaxation times of these materials were long, saturation curves were run on all samples. The details of the

EPR behavior of these centrifuged materials will be described in a separate publication.[14]

9. *Gel Permeation Chromatography*—The high pressure GPC system consisted of a DuPont 850 pumping module connected to a DuPont high temperature column compartment. A Knauer refractive index detector and four μ-styragel columns in series, with maximum sizes of 1000, 500, 500, and 100 Å were used for detection and separation. The GPC eluent was trichlorobenzene heated at 90°C. The separated phases were solubilized for GPC evaluation by reductive ethylation using previously established techniques.[15] Molecular weights were determined from the GPC elution volumes from a calibration curve obtained for separated aromatic pitch fractions.[15]

10. *Polarized Light Microscopy and Mesophase Contents*—Polarized light microscopy was used to determine mesophase contents of the centrifuged pitches. For this purpose, separate centrifuge experiments were carried out utilizing 5 mm O.D. thin-wall Pyrex NMR tubes. The tubes were potted longitudinally in epoxy, ground and polished to the centerline, and examined by polarized light microscopy. The position of the demarcation line was determined by a travelling microscope and the "demarcation line" volumes of the two phases corrected for the small amounts of the trapped inclusions. These were determined by using higher magnification microscopy techniques followed by image analysis. The demarcation line region and trapped phases in the petroleum mesophase pitch are shown in Figure 1.

The total mesophase contents and percentages of mesophase trapped in the isotropic phase and isotropic phase trapped in the mesophase are listed for the three mesophase pitches in Table I. For comparison, the percentages of these pitches insoluble in pyridine (PI) are also included. Approximately one-third of the volume of

TABLE I

Mesophase contents and solubilities of mesophase pitches

Mesophase Pitch	Total Mesophase (Vol. %)	Total Isotropic Phase (Vol. %)	Trapped Phases: Mesophase in Isotropic (Vol. %)	Trapped Phases: Isotropic in Mesophase (Vol. %)	PI (Wt. %)
Petroleum	74.7	25.3	8.5	2.5	54.6
Coal Tar	52.4	47.6	7.0	1.8	50.0
Naphthalene	39.3	60.7	3.7	1.0	42.4

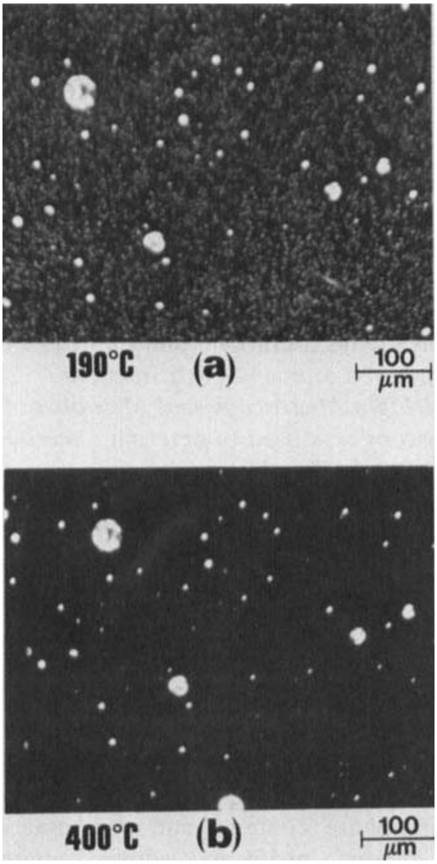

FIGURE 2 Hot-stage photomicrographs of the same region of the isotropic phase of a petroleum mesophase pitch at (a) 190°C and (b) 400°C showing precipitation of mesophase spheres.

mesophase trapped in the isotropic phase was due to spheres precipitated upon cooling from 400°C. This was determined by hot-stage microscopy as shown in Figure 2 for the isotropic phase of the petroleum pitch at 190°C and 400°C. Note that the precipitated sphere size in Figure 2(a) is 5 μm or less.

EXPERIMENTAL RESULTS

The complete characterization data for the separated phases of the three mesophase pitches are summarized in Table II. The differences

TABLE II

Characterization data for separated phases of mesophase pitches

	Naphthalene Mesophase	Naphthalene Isotropic	Petroleum Mesophase	Petroleum Isotropic	Coal Tar Mesophase	Coal Tar Isotropic
He Density (g/cm^3)	1.35	1.29	1.32	1.27	1.36	1.33
% C	96.2	95.3	94.1	93.6	93.9	94.0
% H	4.10	4.37	4.43	4.74	3.83	4.06
Atomic C/H	1.97	1.83	1.78	1.66	2.06	1.94
% N	---	---	0.3	0.3	1.3	1.1
% S	---	---	1.15	1.17	0.48	0.48
T_g (°C) (DSC)	166	116	230	184	220	178
T_g (°C) (TMA)	169	114	225	185	219	173
% Carbon Yield (1000°C)	75.8	61.8	73.6	65.6	74.4	63.5
X-Ray Interlayer Distance (Å)	3.50	3.54	3.52	3.54	3.47	3.54
Spin Concentration (10^{19}/g)	1.24	0.52	1.25	0.51	2.18	0.96
% Toluene Insolubles	83	70	75	68	96	73
Mol. Wt. ($\overline{M}_n$)	989	810	937	840	874	797

between the anisotropic and isotropic phases show the same trends for each of the pitches.

As expected in all cases, the mesophase is more dense than the corresponding isotropic phase. The relative density differences between the phases range from 4.0 to 4.7% for the petroleum and naphthalene pitches to 2.3% for the coal tar pitch. These differences in density are larger than that usually found for the mesophase and isotropic phase of rod-like nematic liquid crystalline materials.[16]

From the elementary analysis data, it is evident that the mesophase has a higher atomic C/H ratio than the co-existing isotropic phase. There is little difference in the distribution of heteroatoms between the two phases.

Both DSC and TMA were used to determine the glass transitions of the separated phases. As a result of their complex nature, pitch materials do not exhibit sharp melting points but transform from a solid to a low viscosity liquid over a wide temperature range. Pitches behave as super-cooled glasses and the glass transition can be detected using both DSC and TMA techniques.[17] Figure 3 presents DSC curves obtained at a fast (200°C/minute) heating rate for the anisotropic and

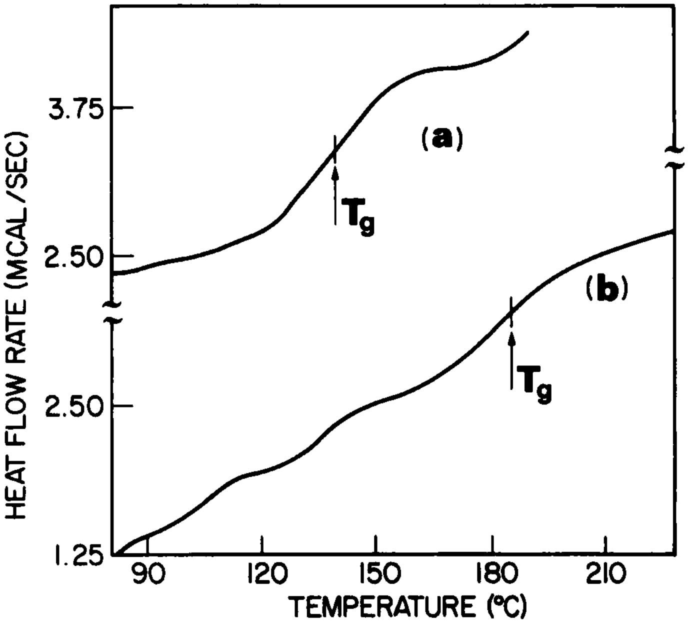

FIGURE 3 DSC traces of (a) isotropic and (b) anisotropic phases of naphthalene mesophase pitch.

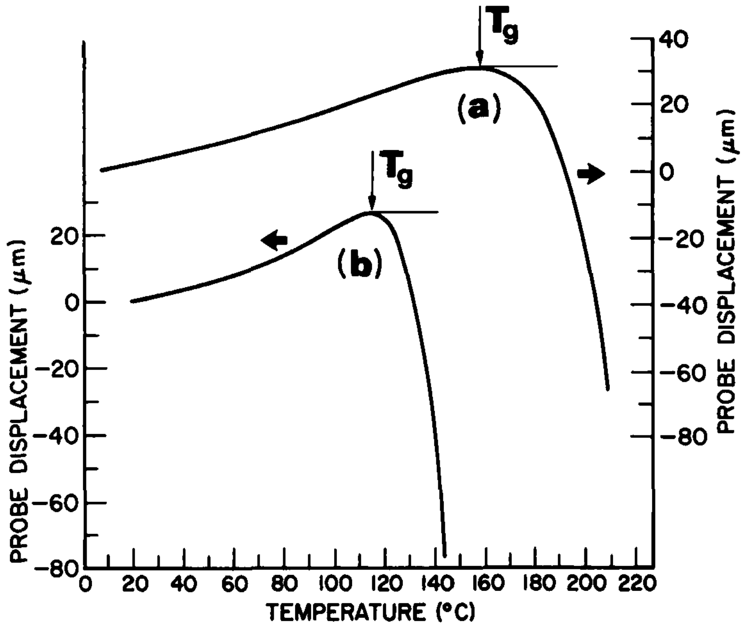

FIGURE 4 TMA curves of probe displacement versus temperature of (a) anisotropic and (b) isotropic phases of naphthalene mesophase pitch.

isotropic phases of the naphthalene-derived mesophase pitch. In order to obtain more accurate glass transition (T_g) temperatures, slower heating rates were used, and the transition midpoints are listed in Table II. The DSC transition midpoints have been reported to give more accurate T_g's for plasticized polymer systems.[18] The T_g's for the mesophases are about 40–50°C higher than those for the corresponding isotropic phases. The TMA penetration curves for the same naphthalene pitch phases are shown in Figure 4. The TMA T_g temperatures were taken at the point of the initial decrease in slope of the curves.[17] These measured T_g values are in good agreement with those from DSC. The T_g data obtained by TMA for all the materials are also summarized in Table II.

The carbon yields obtained by TGA for each fraction are summarized in Table II. As can be seen, the carbon yield of the mesophase is about 8–11% higher than that for the isotropic phase. The lower yields of carbon residue for the isotropic phases reflect their higher contents of lower molecular weight volatile components.

All of the separated phases exhibited X-ray diffraction peaks at a Bragg angle corresponding to a repeat distance of ~3.5Å. This peak

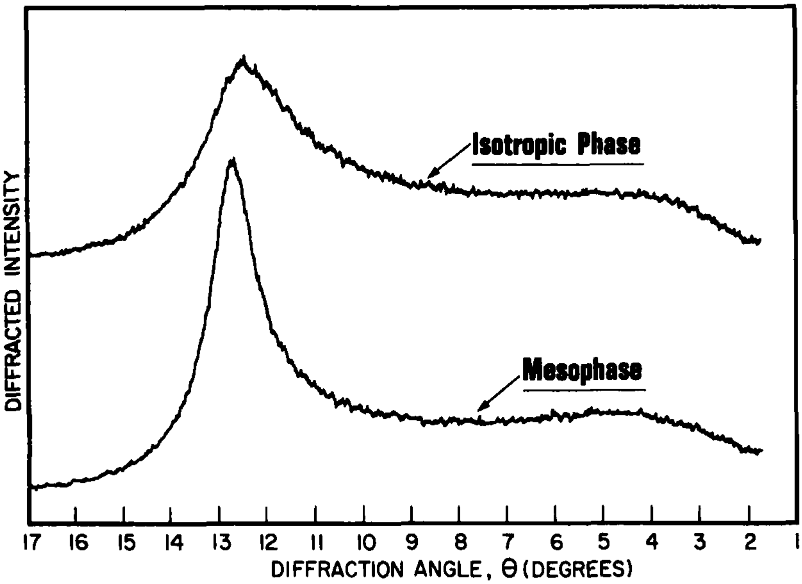

FIGURE 5 X-ray diffraction curves for (a) isotropic and (b) anisotropic phases of petroleum mesophase pitch.

is believed to be associated with the stacking of the discotic aromatic molecules in the pitch and is the predecessor of the conventional 002 peak in carbon and graphite materials. The peak was sharper and occurred at slightly higher angles for the mesophases than for the isotropic phases as shown in Figure 5 for the petroleum pitch. The X-ray interlayer distances for all of the fractions are given in Table II.

EPR curves for the two separated phases of the coal tar mesophase pitch are shown in Figure 6. For all these materials, the lineshapes were intermediate between Gaussian and Lorentzian, with the linewidth (S_F) being somewhat sharper for the anisotropic phases. The relative spin concentrations given in Table II for the separated phases indicate substantially higher values for the anisotropic phases. This is consistent with previous work which indicated an increase in free radical content with molecular weight.[19]

Wide variations in microwave saturation behavior were observed for the different fractions. In Figure 7, saturation curves for the centrifuged phases and the pyridine solubles and insolubles are compared for the naphthalene mesophase pitch. The spin-lattice relaxation times decrease as one proceeds from left to right, indicating

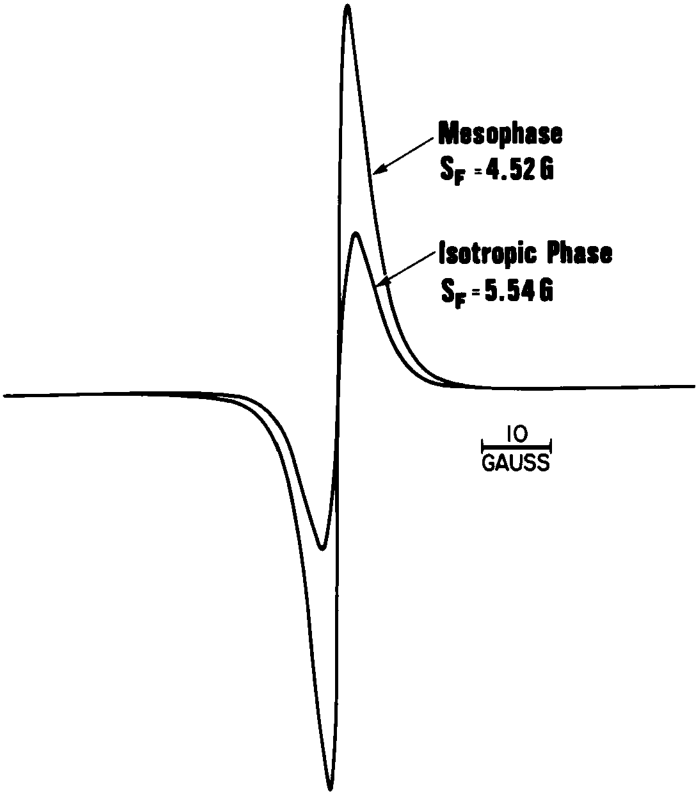

FIGURE 6 EPR curves for equal weights of the two phases of a coal tar-based mesophase pitch.

increasing average free-radical size and concentration as one proceeds from PS to isotropic phase to mesophase pitch to anisotropic phase to PI. It should be noted that saturation can become observable at powers as low as 1 μw.

The molecular weight distributions were measured by GPC for all of the isotropic and anisotropic fractions. Typical curves for the naphthalene pitch fractions are shown in Figure 8. The number average molecular weights, $\overline{M}_n$, tabulated in Table II, demonstrate that the mesophase has a higher average molecular weight than the corresponding isotropic phase, but that the difference is not large. The differences are 97, 77, and 179 for the petroleum, coal tar, and naphthalene pitches, respectively. The relatively high $\overline{M}_n$ of the isotropic phases is consistent with the high percentages of toluene insolubles present in these materials.

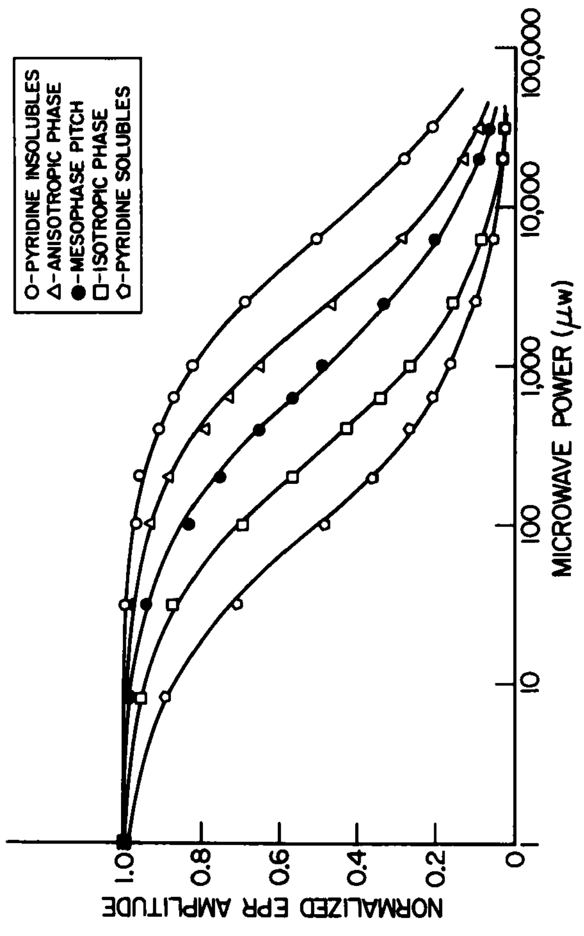

FIGURE 7 EPR saturation curves for different fractions of naphthalene mesophase pitch.

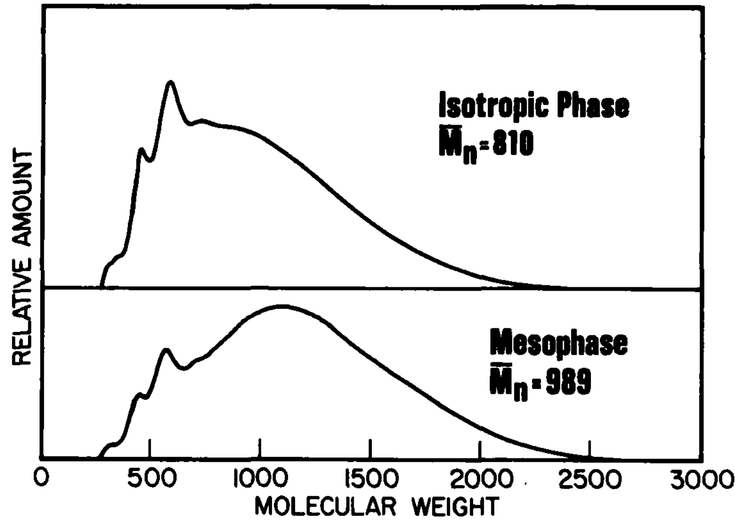

FIGURE 8 GPC molecular weight distribution for separated phases of a naphthalene mesophase pitch.

DISCUSSION

The carbonaceous mesophase is composed of disc-like polynuclear aromatic hydrocarbons and heterocycles with sufficient parallel stacking to form a nematic liquid crystalline phase. Because of its higher density, the ordered mesophase can be separated from the lower density isotropic phase by centrifugation at high temperatures. As can be seen from the analytical results for the separated phases, the chemical differences between the anisotropic and isotropic phases in mesophase pitch are quite subtle. The degree of difference also varies with the nature of the pitch precursor.

The higher C/H ratio and average molecular weight for the mesophase, as compared to the isotropic phase, is consistent with the role of aromatic dehydrogenative polymerization in the formation of mesophase in pitch. As with rod-like liquid crystals, a minimum molecular size is required for the development of mesophase for the polynuclear aromatic components of pitch. However, both molecular weight distribution and molecular size are key factors controlling the development of a mesophase state in pitch.

This conclusion is apparent from the molecular weight data which are presented in Figure 9. Plotted in Figure 9 is the relative partitioning of molecules, as a function of molecular weight, between the

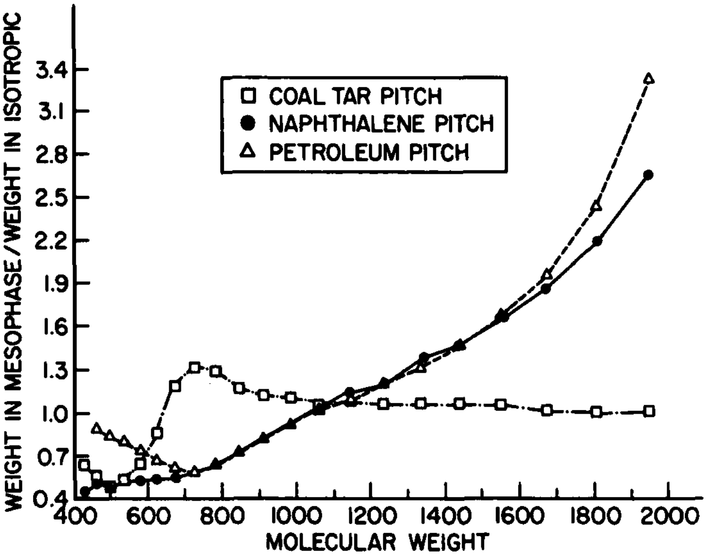

FIGURE 9 Partitioning of molecules in separated pitch phases as a function of molecular weight.

separated phases for each of the three mesophase pitches. This distribution was computed from the GPC curves which were normalized to a constant sample injection weight. As can be seen from the Figure, the anisotropic and isotropic phases contain species with identical molecular weights. However, the mesophase tends to contain a higher concentration of larger molecules and lower concentration of smaller molecules than the isotropic phase. This effect is readily apparent for the naphthalene and the petroleum-derived mesophase where the ratios are 2.8 and 3.4, respectively, for the highest molecular weight range covered. The coal tar pitch appears unique and does not show the continual increase in distribution ratio with increasing molecular size that is evident for the other two materials. The coal tar pitch shows a substantially higher content of low molecular weight molecules (less than 700) in the isotropic phase, but a substantially constant mesophase/isotropic distribution ratio of about 1.2 over the remaining molecular weight range. The cause for this difference is not clear, but could be due to more highly condensed aromatic structures for the coal tar compounds or the greater content of heterocyclic constituents than in the other two materials. Additional studies on mesophase pitches of controlled chemical structure are needed to resolve this question. With the use of high temperature centrifuging techniques, the detailed studies necessary for further clarification of the nature of the isotropic and anisotropic phases in a mesophase pitch are entirely feasible.

Acknowledgment

The authors wish to acknowledge the assistance of D. M. Riffle for sample preparation and EPR measurements.

References

1. J. D. Brooks and G. H. Taylor, "Chemistry and Physics of Carbon," P. L. Walker, Jr., Editor, Marcel Dekker, New York, New York, Vol. **4**, 243 (1968).
2. C. A. Kovac and I. C. Lewis, *Carbon* **16**, 433 (1978).
3. H. Gasparoux, *Mol. Cryst. Liq. Cryst.* **63**, 231 (1981).
4. L. S. Singer and R. T. Lewis, Extended Abstracts, 11th Biennial Conference on Carbon, (1973), pp. 207–208.
5. P. Delhaes, J. C. Rouillon, G. Fug and L. S. Singer, *Carbon* **17**, 435 (1979).
6. H. Marsh and P. L. Walker, Jr., "Chemistry and Physics of Carbon," P. L. Walker, Jr. and P. Thrower, Editors, Marcel Dekker, New York, Vol. **15**, 229–286 (1979).
7. J. E. Zimmer and J. L. White, *Adv. Liq. Cryst.* **5**, 157 (1982).
8. I. Mochida and Y. Korai, *Res. Adv. Carbon Tech.*, J. Ishakowa and T. Nagaoki, Editors, JEC Press, Cleveland, Ohio, p. 361–371 (1983).
9. I. C. Lewis, *Carbon* **20**, 519 (1982).
10. D. M. Riggs and R. J. Diefendorf, Extended Abstracts, 14th Biennial Conference on Carbon, Penn State University, (1979), p. 413.
11. L. S. Singer and D. M. Riffle, To Be Published in Carbon.
12. R. A. Greinke and I. C. Lewis, *Carbon* **22**, 305 (1984).
13. H. A. Friedman, *J. Sci. Instrum.*, **44**, 454 (1967).
14. L. S. Singer, I. C. Lewis and D. M. Riffle, Extended Abstracts, 17th Biennial Conference on Carbon, Lexington, Kentucky, June 16–21, 1985, pp. 155–156. To be published in CARBON.
15. R. A. Greinke and L. H. O'Connor, *Anal. Chem.* **52**, 1877 (1980).
16. G. W. Gray, "Molecular Structure and the Properties of Liquid Crystals," Academic Press, New York, 1962, pp. 112–114.
17. J. B. Barr and I. C. Lewis, *Therm. Chim. Acta.* **52**, 297 (1982).
18. H. E. Bair, "Thermal Characterization of Polymeric Materials," Edited by E. A. Turi, Academic Press, New York, 1981, p. 880.
19. L. S. Singer and I. C. Lewis, *Carbon* **16**, 417 (1978).